Pion emission in α-particle interactions with various targets of nuclear emulsion detector

A. Abdelsalam[1,5] Z. Abou-Moussa[1,5] N. Rashed[2,5] B. M. Badawy[3,5;1)] H. A. Amer[4]
W. Osman[1,5] M. M. El-Ashmawy[4] N. Abdallah[4,5]

[1] Physics Department, Faculty of Science, Cairo University, Giza, Egypt
[2] Physics Department, Faculty of Science, Fayoum University, Fayoum, Egypt
[3] Reactor Physics Department, Nuclear Research Center, Atomic Energy Authority, Egypt
[4] Nuclear and Radiological Regulatory Authority, NRRA, Egypt
[5] Mohamed El-Nadi High Energy Lab, Faculty of Science, Cairo University, Egypt

Abstract: The behavior of relativistic hadron multiplicity for ^{4}He-nucleus interactions is investigated. The experiment is carried out at 2.1 A and 3.7 A GeV (Dubna energy) to search for the incident energy effect on the interactions inside different emulsion target nuclei. Data are presented in terms of the number of emitted relativistic hadrons in both forward and backward angular zones. The dependence on the target size is presented. For this purpose the statistical events are discriminated into groups according to the interactions with H, CNO, Em, and AgBr target nuclei. The separation of events, into the mentioned groups, is executed based on Glauber's multiple scattering theory approach. Features suggestive of a decay mechanism seem to be a characteristic of the backward emission of relativistic hadrons. The results strongly support the assumption that the relativistic hadrons may already be emitted during the de-excitation of the excited target nucleus, in a behavior like that of compound-nucleus disintegration. Regarding the limiting fragmentation hypothesis beyond 1 A GeV, the target size is the main parameter affecting the backward production of the relativistic hadron. The incident energy is a principal factor responsible for the forward relativistic hadron production, implying that this system of particle production is a creation system. However, the target size is an effective parameter as well as the projectile size considering the geometrical concept regarded in the nuclear fireball model. The data are analyzed in the framework of the FRITIOF model.

Key words: α-particle interactions at Dubna energies, shower particle sources, target size dependence, FRITIOF model

PACS: 25.75.-q, 25.75.Dw, 25.75.Gz **DOI:** 10.1088/1674-1137/39/9/094001

1 Introduction

In low-energy nuclear collisions, the particle production mechanism can be accounted for fairly well by one single source. De-excitation can be understood in terms of particle emission from a liquid drop of nuclear matter. At high energy, multiple sources are needed. The de-excitation is here understood in terms of particle emission from an expanding gas of nuclear matter in thermodynamical equilibrium. At excitation energies comparable with the total binding energy, $\sim$5 A to 8 A MeV, the very existence of a long-lived compound nucleus becomes unlikely. In this situation an explosion-like process leads to the total disintegration of the nucleus and the multiple emission of nuclear fragments of different masses [1 and references therein]. One can come to the multifragmentation concept from quite a different starting point, by considering a liquid-gas phase transition in excited nuclear matter. The name "multifragmentation" is introduced firstly in Ref. [2]. Ma's law, the so-called nuclear Zipf's law, can give the possible phase change signal using the fragment rank distribution [3]. Dabrowska et al. study the multifragmentation of Pb at 158 A GeV in comparison with that of Au at 0.64 A and 10.6 A GeV [4]. The results suggest that multifragmentation is nearly energy independent at $E_{\rm lab}\geqslant$10 A GeV. They apply the nuclear Zipf's law to multifragmentation events, where it roughly agrees with the data. This evidences the existence of the critical temperature associated with a liquid-gas phase transition. Ma et al. [5] investigate the critical behavior in light nuclear systems, where the excitation energy ranges from 1 A up to 9 A MeV. At an excitation energy $\sim$5.6 A MeV and a temperature $\sim$8.3 MeV, the presence of maximal fluctuations in the

Received 6 February 2015
1) E-mail: he_cairo@yahoo.com

de-excitation processes is observed. At this point the fragment distributions are associated with criticalities which are very close to those of the liquid-gas phase transition universality. The fragment topological structure shows that the rank-sorted fragments obey the nuclear Zipf's law at the largest fluctuation point, providing another indication of the liquid-gas phase transition. In high energy collisions, the produced particles are not confined to nuclear fragments but they include essentially created particles, the so-called hadrons.

On the other hand, the high-energy hadron–hadron, hadron–nucleus, or nucleus–nucleus interactions are a precise source in which all categories of secondary emitted particles are available. It is very important to learn as much as possible about all the phenomena which occur in these interactions, to observe the anticipated signatures in the background of "normal phenomena". Some of these phenomena are hadron production, projectile fragmentation, target fragmentation, multiplicity and emission characteristics, reaction cross sectional behavior, and stopping power of the target materials in the detector with respect to each passing particle. Hence, the choice of projectiles, targets, energies, and critical parameters in measurements motivates the correct modeling and simulation of the experiments. The synchrophasotron accelerator at Dubna enables equipping beams of $A \geqslant 1$, in a few A GeV range of energies. This region is a special energy range, in which the nuclear limiting fragmentation applies initially [6–12]. Nuclear emulsion is a very useful tool in experimental physics for investigating atomic and nuclear processes. It can be used as a detector of 4-πspace geometry. It contains target materials over a wide range of mass numbers, ^{1}H, ^{12}C, ^{14}N, ^{16}O, ^{82}Br, ^{108}Ag. It has the possibility of measuring energies and angles with a high degree of resolution. It can be used in studying the characteristics of new elementary particles and can detect the decay of unstable neutral particles, its sensitivity to slow charged particles arising from the disintegration of the target nucleus. Owing to the high stopping power of emulsion, a large fraction of short-lived particles is brought to rest in it before decay and hence their ranges and lifetimes can be measured accurately.

In this work the interactions of α-particles with emulsion nuclei are studied at Dubna energies (2.1 A and 3.7 A GeV), focusing on the investigation of relativistic hadron (shower particle) production, according to emission angular zone and target size effect.

2 Experimental details

The NIKFI-BR2 nuclear emulsion stacks used in this experiment were irradiated by α–particle beams at the JINR Synchrophasotron in Dubna, Russia. The beam energies are 2.1 A and 3.7 A GeV. Each emulsion pellicle size is 20 cm×10 cm × 0.06 cm. Table 1 shows the chemical composition of this emulsion type.

Table 1. Chemical composition of NIKFI-BR2 emulsion.

element	^{1}H	^{12}C	^{14}N	^{16}O	^{80}Br	^{108}Ag
atoms/cm^3×10^{22}	3.150	1.410	0.395	0.956	1.028	1.028

The methods used, equipment, and experimental restrictions are similar to the experiments detailed in Refs. [13, 14].

The produced particles are identified in photographic nuclear emulsion according to the commonly accepted ionization behavior [15, 16], as:

1) Shower particles with $g \leqslant 1.4 g_{\rm p}$ where g is the track grain density and $g_{\rm p}$ corresponds to the grain density of the minimum ionizing track. These particles are relativistic hadrons, which consist mainly of pions and less than 10% mesons and baryons. Their multiplicity is denoted as $n_{\rm s}$. The notations $n_{\rm s}^{\rm f}$ and $n_{\rm s}^{\rm b}$ correspond to the shower particles emitted in the forward hemisphere, FHS, within $\theta_{\rm lab} < 90^\circ$ and in the backward hemisphere, BHS, within $\theta_{\rm lab} < 90^\circ$ within $\theta_{\rm lab} < 90^\circ$, respectively.

2) Grey particles with a range >3 mm and $1.4 g_{\rm p} < g \leqslant 4.5 g_{\rm p}$; they are mainly recoil protons knocked out from the target nucleus during the collision. Their kinetic energy ranges from 26 to 400 MeV.

3) Black particles with a range $\leqslant$3 mm and $g > 4.5 g_{\rm p}$; they are evaporated target protons with kinetic energy <26 MeV.

4) The grey and black particles together are the group of target fragments, the so called heavily ionizing particles. These fragments are emitted in 4-π space. Their multiplicity is denoted as $N_{\rm h}$.

5) Projectile fragments with $Z \geqslant 1$; they are fragmented nuclei with nearly the same momentum as the incident nucleus. They are emitted in a very narrow forward cone along the direction of incidence.

3 Results and discussion

3.1 Interaction cross-section

Listed in Table 2 are the total scanned lengths, L, of the primary beam tracks; the number of resulting inelastic interactions, N; and the corresponding average values of the experimental mean free path, λ. The mean free path of α-particles in the NIKFI-BR2 emulsion type is predicted using a Glauber's approach simulation code [17] as 18.79 cm. It is concluded from Table 2 that the mean free path of α-particles in nuclear emulsion is not sensitive to the energy where the measured and predicted values are nearly in agreement with each other.

Since the nuclear emulsion is a homogeneous mixture of different nuclei, the inelastic interactions can be classified into groups according to the target nucleus. In

this experiment the event discrimination is executed using the widely explained methods [14] and [18–22] and the theoretical predictions of Glauber's approach [17]. The present inelastic interactions cross sections are correlated with the target mass number in Fig. 1. From Fig. 1, the cross sectional values are nearly the same at the two-energies used. Glauber's approach can predict them well. The data are approximated by the power law relation of Eq. (1), which is presented by the smooth curves in Fig. 1. The fit parameters, α and β, are listed in Table 3. The fit parameters are $\alpha\sim120$ and β=0.56–2/3. Therefore, Eq. (1) can be rewritten as Eq. (2).

$$\sigma=\alpha A_{\rm T}^{\beta}, \tag{1}$$

$$\sigma=120A_{\rm T}^{0.56}\ {\rm mb}. \tag{2}$$

Table 2. Beam interaction data.

$E_{\rm lab}/A$ GeV	L/m	N events	λ/cm
2.1	416.5	2066	20.16±0.44
3.7	217.6	1092	19.93±0.60

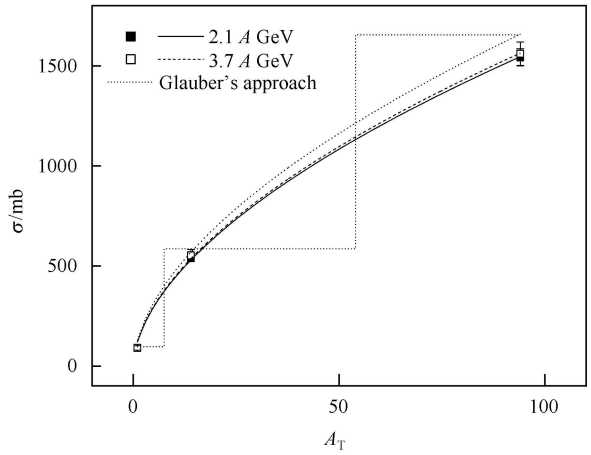

Fig. 1. Cross section of the present α-particle inelastic interactions in nuclear emulsion as a function of the target size, together with the predictions of Glauber's approach (histogram).

Table 3. Fit parameters of Eq. (1).

fit parameter	α	β
$E_{\rm lab}$=2.1 A GeV	119.74±16.43	0.56±0.03
$E_{\rm lab}$=3.7 A GeV	121.46±17.10	0.56±0.03
Glauber's approach prediction	128.54±17.88	0.56±0.03

3.2 Multiplicity distributions

In what follows, the inelastic interaction samples of 2.1 A and 3.7 A GeV α-particle in nuclear emulsion are separated into statistical groups according to the target sizes. Applying the predicted percentages of Glauber's theory encoded in Ref. [17], we categorize the data according to the interactions with H, CNO, Em, and AgBr targets separately. The effective mass number of each target group of nuclei is 1, 14, 70, and 94, respectively. A modified FRITIOF code is used to simulate the present data. It is based on the Lund version 1.6 [22, 23]. The modification was carried out by V. V. Uzhinskii, LIT, JINR, Dubna, Russia, in 1995. The predictions of the model are presented in the enclosed figures by histograms and are placed between round brackets throughout the tables.

In Fig. 2 the backward emitted shower particle multiplicity distributions associated with the present interactions are shown.

$$P(n_{\rm s}^{\rm b})=p_{\rm s}^{\rm b}{\rm e}^{-\lambda_{\rm s}^{\rm b}n_{\rm s}^{\rm b}}. \tag{3}$$

For all targets, the characteristic feature of the distribution is the exponential decay shape. The multiplicity range (decay tail) increases with the target size. For α-particles, as light projectiles, the energy seems to have a qualitatively considerable effect. This effect is reflected on the longer distributions' tails at 3.7 A GeV than at 2.1 A GeV. The characteristic exponential behavior can be approximated by Eq. (3). The fit parameters, $P_{\rm s}^{\rm b}$ and $\lambda_{\rm s}^{\rm b}$, are listed in Table 4. The data are reproduced well by the model. The exponential fit of the experimental data and their theoretical predications are presented by the solid and dashed curves, respectively. In Table 4, the fit parameters are affected weakly by energy. The small energy effect consists of a longer decay tail of the distributions at 200 A GeV than at 3.7 A GeV. This effect is attributed to more excitation in the target nucleus at the higher energy. Consequently, the produced compound nucleus will de-excite and decay by emitting this excess number of backward hadrons. Such a mechanism for compound target nuclei was discussed in experiments [24, 25]. Therefore, regarding the nuclear limiting fragmentation beyond 1 A GeV, the projectile energy cannot be considered an effective parameter in the backward production and consequently does not mean that this system of particle production is a creation system. The values associated with the model in Table 4 often agree with the measured ones.

The backward emitted shower particle multiplicity at the two incident energies can be determined as a function of the effective target mass, $A_{\rm T}$, as in Fig. 3.

Therefore, the fit parameters of Table 4 are correlated with $A_{\rm T}$. The linear fitting is approximated by Eq. (4) and Eq. (5) and presented by the straight lines. The solid and dashed lines belong to the correlation associated with the measured data and their theoretical predictions, respectively. The fit parameters of Eq. (4) and Eq. (5) are shown in Table 5. The slope and intercept parameters decrease linearly with the target mass. Therefore, the backward emission of the relativistic hadron strongly

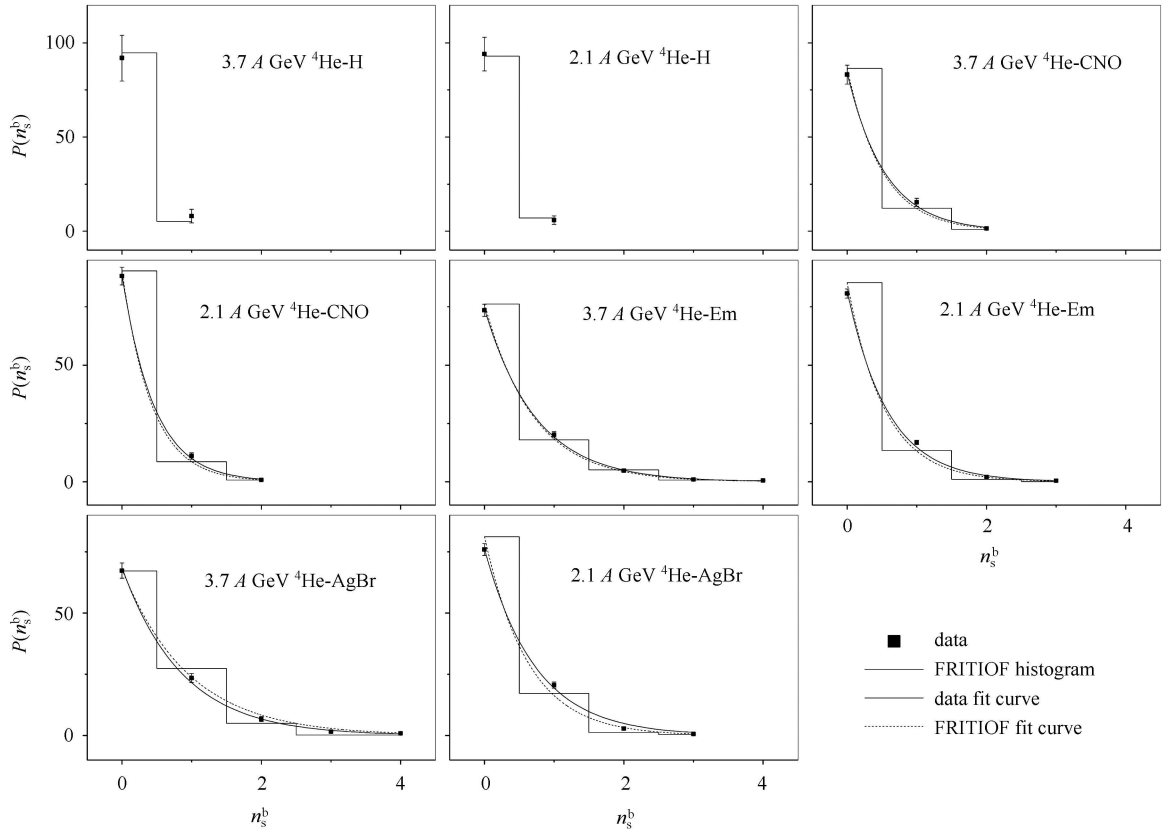

Fig. 2. Multiplicity distributions of the backward shower particles emitted in 2.1 A and 3.7 A GeV ^{4}He interactions with H, CNO, Em, and AgBr nuclei, together with the predictions of the modified FRITIOF model and the exponential decay fitting.

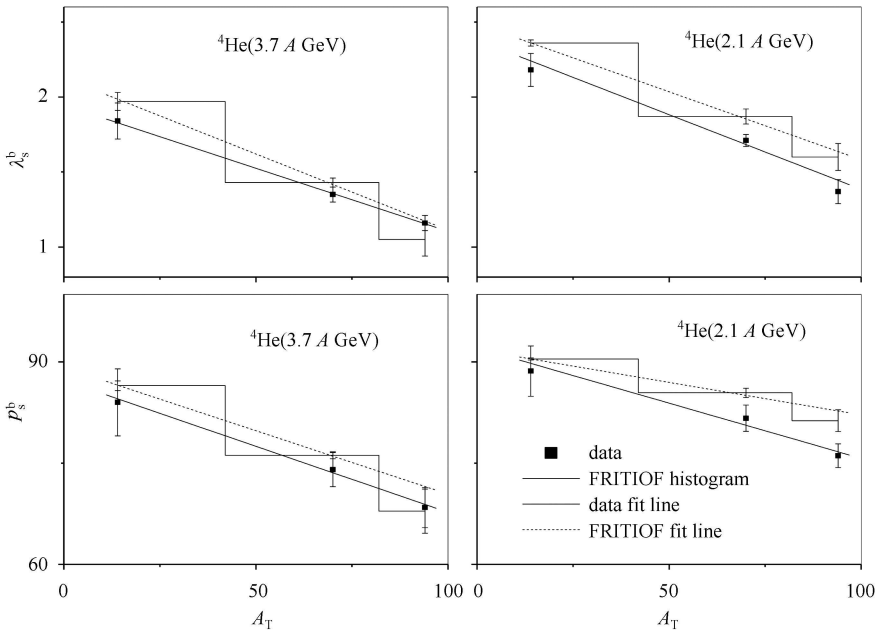

Fig. 3. Fit parameters of Eq. (3) as a function of the target size.

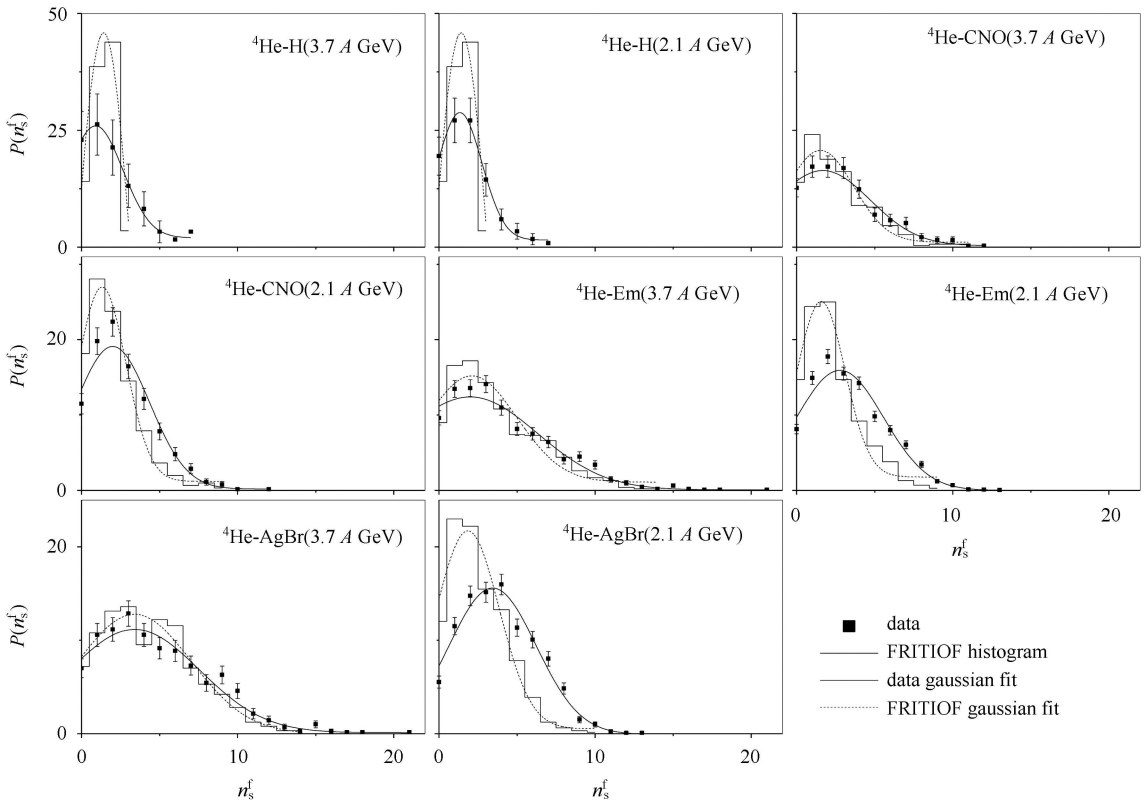

Fig. 4. Multiplicity distributions of the forward emitted shower particle in 2.1 A and 3.7 A GeV ^{4}He interactions with H, CNO, Em, and AgBr nuclei, together with the predictions of the modified FRITIOF model and the Gaussian fitting.

Table 4. Fit parameters of Eq. (3). The numbers in brackets are the predictions of the modified FRITIOF model.

$E_{\rm lab}/A$ GeV	target	$\lambda_{\rm s}^{\rm b}$	$P_{\rm s}^{\rm b}$
2.1	CNO	2.18±0.11	88.64±3.73
		(2.36±0.02)	(90.43±0.15)
	Em	1.71±0.04	81.65±1.95
		(1.87±0.05)	(85.42±0.69)
	AgBr	1.37±0.08	76.10±1.75
		(1.60±0.09)	(81.29±1.61)
3.7	CNO	1.84±0.12	84.00±4.96
		(1.97±0.06)	(86.48±0.71)
	Em	1.35±0.05	74.04±2.52
		(1.43±0.03)	(76.17±0.51)
	AgBr	1.16±0.05	68.44±2.98
		(1.05±0.11)	(67.90±3.28)

depends on the target size.

$$\lambda_{\rm s}^{\rm b} = a_\lambda + b_\lambda A_{\rm T}, \quad (4)$$

$$P_{\rm s}^{\rm b} = a_{\rm p} + b_{\rm p} A_{\rm T}. \quad (5)$$

In Fig. 4 the forward emitted shower particle multiplicity distributions of the present interactions are shown.

Unlike the observed behavior of the backward emitted shower particles, the characteristic feature here is the peaking curve shapes. In Fig. 4 the multiplicity range as well as the broadening of the distributions increases with target size as well as energy. The geometrical model considering the overlap size between target and projectile seems to be effective in drawing the characteristic features of the distributions. Accordingly the effect of the target size is reflected in the impact parameter value and consequently in the energy participation, which is the main effective parameter in particle creation. The

Table 5. Fit parameters of Eq. (4) and Eq. (5). The numbers in brackets are the predictions of the modified FRITIOF model.

$E_{\rm lab}/A$ GeV	2.1	3.7
a_λ	2.38±0.15	1.95±0.02
	(2.49±0)	(2.13±0.09)
b_λ	−0.01±0	−0.01±0
	(−0.0±0)	(−0.0±0)
$a_{\rm p}$	92.07±0.07	87.27±1.42
	(91.78±0.25)	(89.18±1.02)
$b_{\rm p}$	−0.16±0.04	−0.20±0.02
	(−0.10±0.01)	(−0.19±0.02)

modified FRITIOF model overestimates the data associated with the H target nuclei as well as for those associated with all targets at 2.1 A GeV. The model can reproduce the distributions at 3.7 A GeV for all targets beyond hydrogen. Both the experimental and theoretical distributions are fitted well by the Gaussian shapes presented by the smooth solid and dashed curves, respectively. Thus, it is reasonable to say that the mechanism in this system of particle production in the FHS is completely different from that in the BHS.

3.3 Production probability of pions in BHS

The percentage probability of the backward emitted shower particle production, $P(n_s^b>0)\%$, is defined as the number of events having $(n_s^b>0)$ normalized to the total sample of events. In Fig. 5 this probability is evaluated as a function of the target mass number for the present interactions.

From Fig. 5, one observes the strong dependence of backward relativistic hadron production on the target size. This strong dependence is evaluated linearly by Eq. (6) and presented in Fig. 5 by the straight lines. Independent of the projectile size ($A_{\rm Proj}$ = 1 to 32) or energy ($E_{\rm lab}$=2.1 A to 200 A GeV), backward relativistic hadrons are produced with probability values of ∼20% to 30% for interactions with Em target [26]. The theoretical predictions of the FRITIOF model agree with the data, especially at 3.7 A GeV. The fit parameters μ and ν are listed in Table 6.

$$P(n_s^b>0)\%=\mu+\nu A_T. \quad (6)$$

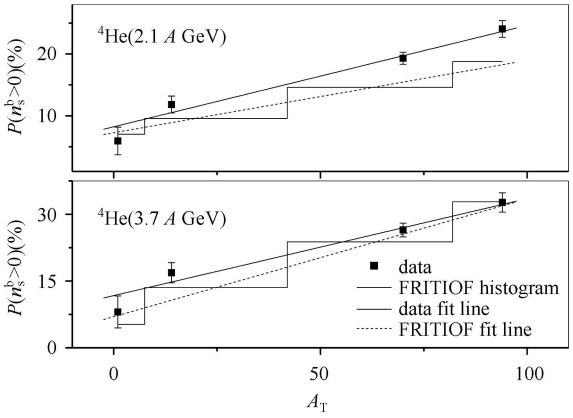

Fig. 5. Probability of the backward emitted shower particle multiplicity, in the interactions of 2.1 A and 3.7 A GeV ^{4}He with emulsion nuclei, as a function of the target mass number, together with the predictions of the modified FRITIOF model and the fitting lines.

Table 6. Fit parameters of Eq. (6). The numbers in brackets are the predictions of the modified FRITIOF model.

$E_{\rm lab}/A$ GeV	μ	ν
2.1	8.22±1.42 (7.26±0.69)	0.16±0.02 (0.12±0.01)
3.7	11.72±2.22 (6.99±2.16)	0.22±0.03 (0.27±0.04)

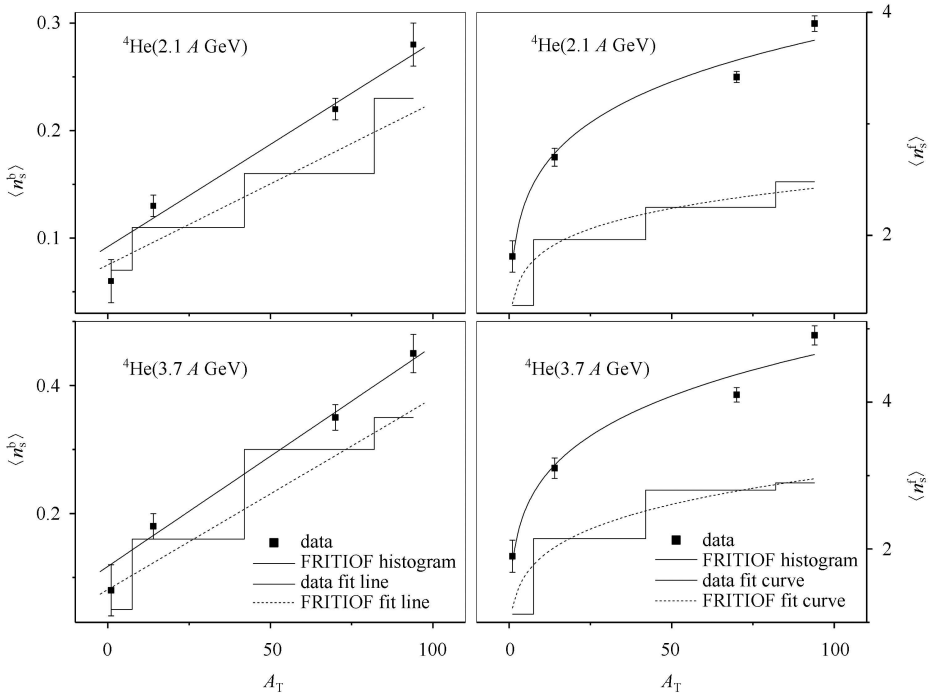

Fig. 6. Dependence correlations of the forward and backward emitted shower particle average multiplicities on the target size in the present interactions, together with the theoretical prediction.

Table 7. Fit parameters of Eq. (7) and Eq. (8). The numbers in brackets are the predictions of the modified FRITIOF model.

$E_{\rm lab}/A$ GeV	$a_{\rm s}^{\rm b}$	$b_{\rm s}^{\rm b}$	$a_{\rm s}^{\rm f}$	$b_{\rm s}^{\rm f}$
2.1	0.092±0.016 (0.075±0.016)	0.002±0 (0.002±0)	1.77±0.13 (1.39±0.07)	0.17±0.02 (0.12±0.01)
3.7	0.117±0.020 (0.081±0.029)	0.003±0 (0.003±0)	1.83±0.23 (1.20±0.09)	0.21±0.03 (0.20±0.02)

3.4 Average multiplicity

The average multiplicities of the forward and backward shower particles, emitted in the present interactions, are correlated with the target size in Fig. 6. The correlation reveals a linear dependence for the backward emitted shower particles, presented by the straight lines. Eq. (7) approximates the values of fit parameters, $a_{\rm s}^{\rm b}$ and $b_{\rm s}^{\rm b}$, which are listed in Table 7. The model reproduces the linear correlation especially at 3.7 A GeV. The slope parameter $\sim$0 and the intercept parameter $\sim$ 0.1, irrespective of the energy.

$$\langle n_{\rm s}^{\rm b}\rangle = a_{\rm s}^{\rm b} + b_{\rm s}^{\rm b} A_{\rm T}. \quad (7)$$

In experiment [26], using a wide range of projectile size ($A_{\rm Proj}$=1 to 32) interacting in nuclear emulsion at Dubna energy, the values of $\langle n_{\rm s}^{\rm b}\rangle$ are found to increase with projectile size for $A_{\rm Proj}<6$. At $A_{\rm Proj}\geqslant 6$, they began to saturate and had a constant value of $\langle n_{\rm s}^{\rm b}\rangle\sim 0.4$. In this experiment the results imply that the energy is not an effective parameter in backward shower emission. Therefore, one can conclude that, while the average shower particle multiplicity, emitted in the BHS, depends on the target size, it depends neither on the projectile size nor energy. This confirms our expectation that the backward relativistic hadrons do not come from the fireball nuclear matter or hadronic matter. They are target source particles, regarding the nuclear limiting fragmentation regime. In Fig. 6, the forward emitted shower particle average multiplicity shows higher values than the backward ones. It increases with the energy as well as target size. The increase with the target size here does not mean that this particle is a target source, but the target size enhances the total system size which affects the participant matter size. Although the dependence on the target size is strong, it has a tendency to saturate at $A_{\rm T}>14$. This behavior may be reflected on the dependence which is approximated well by the power law relation of Eq. (8). This approximation is presented in Fig. 6 by the smooth curves. The fit parameters, $a_{\rm s}^{\rm f}$ and $b_{\rm s}^{\rm f}$, are listed in Table 7. From Fig. 6, one can also observe that the model underestimates the data. Abdelsalam et al. [26] determine the dependence of $\langle n_{\rm s}^{\rm f}\rangle$ on the projectile mass number at Dubna energy. They find that dependence to be: $\langle n_{\rm s}^{\rm f}\rangle = 1.89\ A_{\rm proj}^{0.56}$, i.e. $\langle n_{\rm s}^{\rm f}\rangle \propto r_{\rm proj}^{2/3}$.

$$\langle n_{\rm s}^{\rm f}\rangle = a_{\rm s}^{\rm f} A_{\rm T}^{b_{\rm s}^{\rm f}}. \quad (8)$$

Comparing this dependence with Eq. (8), it can be observed that the majority contribution of the participant matter is accounted for by the projectile throughout the production of the forward emitted shower particles. Thus, while the production source of the backward emitted shower particles is the target fragmentation system, the forward emitted particles originate mainly from a creation system provided by the participant energy.

4 Conclusions

From the analysis of 2.1 A and 3.7 A GeV α-particle interactions, using photographic nuclear emulsion detector, we conclude the following:

1) The inelastic interaction cross section of α-particles in nuclear emulsion is approximated as a function of the target mass number. In the present energy region, the cross section is independent of the energy. It can be determined in the light of Glauber's multiple scattering theory.

2) The dominant mechanism characterizing the backward shower particle production is the decay behavior. There is no energy effect on the backward production. The multiplicity distribution of this hadron is expressed in terms of the target size. While the production probability of these hadrons is independent of the projectile size or energy, it increases linearly with the target size. While the average backward shower particle multiplicity tends to a limited value $\sim$0.4, irrespective of the projectile size or energy, it increases linearly with the target size. Hence, the main effective parameter is the target size, regarding the nuclear limiting fragmentation beyond 1 A GeV. Thus, such hadrons are expected to decay through the de-excitation of the excited target nucleus, similar to the compound nucleus mechanism.

3) In the FHS the shower particle multiplicity distributions are peaking shaped, and can be described well by Gaussian shapes. The production of the forward emitted relativistic hadrons is attributed to a mechanism which is completely different to that in the BHS. Although the target nucleus is not the source of the forward relativistic hadrons, the target size is an effective parameter in this production as well as the projectile size. The geometrical concept underlying the nuclear fireball model may interpret the effect of the projectile and target sizes in particle production at high energy. The effect of the target size on forward shower particle production is reflected in their multiplicity characteristics at each target. Regarding the incident energy role as a principal param-

eter affecting forward relativistic hadron production, this system of production is regarded as a particle creation system, in which the particles are sourced from hadronic matter or fireball nuclear matter.

4) The modified FRITIOF model can predict the system of the relativistic hadron production in the BHS well. In the FHS the hadronization system can be described satisfactorily. This suggests that the Reggeon picture can be considered as a plausible development to the model. Sometimes underestimations or overestimations are observed in the model predictions with experimental data. This may require a modern approach in describing nuclear cascading.

We owe much to Vekseler and Baldin High Energy Laboratory, JINR, Dubna, Russia, for supplying us the photographic emulsion plates irradiated at the Synchrophasotron.

References

1 Bondorf J P, Botvina A S, Iljinov A S, Mishustin I N, Sneppen K. Phys. Rep., 1995, **57**: 133
2 Bondorf J P. Journal de Physique, 1976, **37/C5**: 195; Proceeding of the EPS Topical Conference on Large Amplitude Collective Nuclear Motions, Keszthely, Hungary, June 1979
3 MA Y G. Phys. Rev. Lett., 1999, **83**: 3617
4 Dąbrowska A, Szarska M, Trzupek A, Wolter W, Wosiek B. Acta Physica Polonica B, 2001, **32**: 3099
5 MA Y G et al. Phys. Rev. C, 2005, **71**: 054606
6 Benecke J, CHOU T T, YANG C N, YEN E. Phys. Rev., 1969, **188**: 2159
7 LIU Fu-Hu. Chinese Journal of Physics, 2002, **40**: 159
8 Ahmad M S, Khan M Q R, Hasan R. Nucl. Phys. A, 1989, **499**: 821
9 Webber W R. Proceedings of the International Cosmic Ray Conference, Vol. 8, P. 65, Moscow, USSR. 1987
10 Lindstorm P L, Greiner D E, Heckman H H, Cork B. Lawrence Berkeley Laboratory Report, LBL-3650. 1975
11 Olson D L, Berman B L, Grenier D E, Heckman H H, Lindstrom P J, Crawford H J. Phys. Rev. C, 1983, **28**: 1602
12 El-Nagdy M S, Abdelsalam A, Abou-Moussa Z, Badawy B M. Can. J. Phys., 2013, **91**: 737
13 Abdelsalam A, Metwalli N, Kamel S, Aboullela M, Badawy B M, Abdallah N. Can. J. Phys., 2013, **91**: 438
14 Abdelsalam A, Badawy B M, Hafiz M. J. Phys. G: Nucl. Part. Phys.,2012, **39**: 105104
15 Powell C F, Fowler F H, Perkins D H. The Study of Elementary Particles by the Photographic Method, Pergamon Press. London; New York, Paris, Los Angles, 474. 1958
16 Barkas H. Nuclear Research Emulsion, Vol. I, Technique and Theory Academic Press Inc., 1963
17 Shmakov S Yu, Uzhinskii V V. Com. Phys. Comm., 1989, **54**: 125
18 Florian J R et al. Report Submitted to the Meeting of Division of Particles and Fields, Berkeley, California. 1973
19 Abdelsalam A. JINR Report (Dubna), 1981, E1-81-623
20 Abdrahmanov E O et al. Z. Phys. C, 1980, **5**: 1
21 Adamovich M I et al. (for EMU01 collaboration). Lund University Report, Sweden, LUIP 8904. 1989
22 Andersson B Gustafson G, Nilsson-Almqvist B. Nucl. Phys. B,1987, **281**: 289
23 Nilsson-Almqvist B, Stenlund E. Comp. Phys. Comm., 1987, **43**: 387
24 Abdelsalam A, Shaat E A, Ali-Mossa N, Abou-Mousa Z, Osman O M, Rashed N, Osman W, Badawy B M, El-Falaky E. J. Phys. G: Nucl. Part. Phys., 2002, **28**: 1375
25 Abdelsalam A, Badawy B M, El-Falaky E. Can. J. Phys., 2007, **85**: 837
26 Abdelsalam A, El-Nagdy M S, Badawy B M; Can. J. Phys., 2011, **89**: 261